JOURNAL OF CHEMICAL & ENGINEERING DATA

ARTICLE

pubs.acs.org/jced

Thermodynamic Consistency Test for Experimental Solubility Data in Carbon Dioxide/Methane + Water System Inside and Outside Gas Hydrate Formation Region

Ali Eslamimanesh,[†] Amir H. Mohammadi,[*,†,‡] and Dominique Richon[†]

[†]MINES ParisTech, CEP/TEP - Centre Énergétique et Procédés, 35 Rue Saint Honoré, 77305 Fontainebleau, France

[‡]Thermodynamics Research Unit, School of Chemical Engineering, University of KwaZulu-Natal, Howard College Campus, King George V Avenue, Durban 4041, South Africa

Supporting Information

ABSTRACT: Accurate knowledge of solubility in carbon dioxide/methane + water system over wide ranges of temperatures and pressures is essential for the petroleum industry. However, experimental measurements of such solubilities (especially in gas hydrate formation region) are challenging. For instance, concentrations of these gases in water are low, and furthermore reaching the equilibrium conditions near and inside gas hydrate formation region is a time-consuming process. Those difficulties may consequently result in generation of unreliable experimental data. This work aims at performing a thermodynamic consistency test based on an area approach to study the reliability of such experimental data reported in the literature and points out the suspected inconsistent data. A thermodynamic model based on the Valderrama modification of the Patel-Teja equation of state along with non-density dependent mixing rules is used to model the solubilities in the gas/vapor and liquid water phases. For modeling the solubility of carbon dioxide/methane in water under liquid water-hydrate equilibrium conditions, the van der Waals-Platteeuw model accompanied with Henry's law approach is employed. The results show that about 23 % of all of the investigated experimental data seem to be thermodynamically consistent, 57 % inconsistent, and 20 % not fully consistent data.

INTRODUCTION

Carbon dioxide/methane and water systems are one of major systems in the petroleum industry.[1] Such mixtures are often found in oil and gas streams and reservoirs especially as part of enhanced oil recovery (EOR) process. The presence of carbon dioxide/methane and water in these environments may cause complications such as corrosion and gas hydrate formation.[1] On the other hand, CO_2 capture from industrial/flue gases, and CO_2 sequestration are among the novel technologies dealing with mixtures of these compounds.[2,3] Therefore, because of the fact that the aforementioned processes deal with a wide range of pressures and temperatures, accurate knowledge of the solubility in the carbon dioxide/methane + water system over a wide range of temperatures and pressures are especially necessary to tune adapted thermodynamic models.

Figure 1 shows a typical solubility—temperature diagram for a water—pure hydrate former (limiting reactant) system.[2] As can be seen, the temperature and pressure dependencies of the pure hydrate former (e.g., carbon dioxide and methane) solubility in pure water being in the liquid water—gas/vapor (L_w-G/V depending on whether the component is in supercritical state or not) equilibrium region are different from the corresponding dependency in the liquid water—hydrate (L_w-H) equilibrium region.[2−20] The L_w-G/V equilibrium is a strong function of temperature and pressure, while the L_w-H equilibrium is a strong function of temperature but a very weak function of pressure.[2−20] On the other hand, the pure hydrate former solubility in pure water in the L_w-G/V equilibrium region generally increases with decreasing the temperature at a given pressure, while the corresponding solubility in pure water in the liquid water—hydrate equilibrium region decreases with decreasing the temperature at the same pressure.[2−20] Furthermore, the metastable liquid water—vapor equilibrium may extend well into the gas hydrate formation zone.[2−20]

As pointed out earlier,[1] low solubilities of carbon dioxide/methane gases in water (especially methane) result in some significant experimental measurement difficulties. Although many experimental works have been done to obtain solubilities of carbon dioxide/methane in water in L_w-G/V region, the experimental data for describing the L_w-H equilibrium are limited mainly due to two factors: the possible extension of the metastable L_w-G/V equilibrium into the gas hydrate region and the experimental restraint that the existing analytical methods require modifications.[2−20] Literature surveys reveal the availability of few sets of experimental data for the L_w-H equilibrium.[2−20] Consequently, few reliable models are available in the literature for representing the L_w-H equilibrium data.[2−20] These models are generally based on cubic equations of state, different mixing rules, and mathematical correlations.

To check the existing thermodynamic models or develop new ones, if necessary, for an accurate estimation of the solubility in the carbon dioxide/methane + water system, reliable experimental data sets are required. This communication aims at testing the thermodynamic consistency of such literature solubility data in the wide range of available temperatures and

Special Issue: John M. Prausnitz Festschrift

Received: November 17, 2010
Accepted: February 16, 2011
Published: March 30, 2011

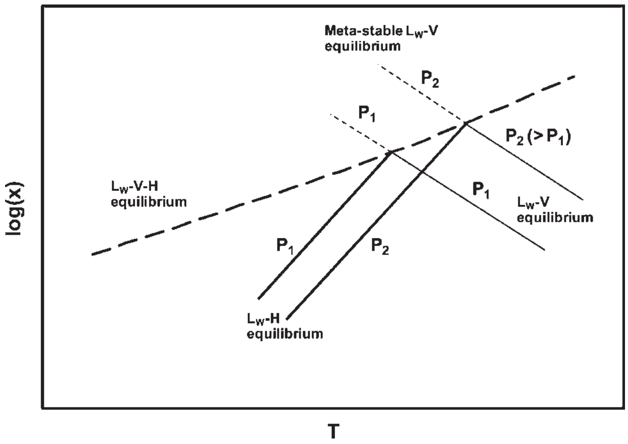

Figure 1. Typical solubility (x)−temperature (T) diagram for water and single (pure) hydrate former (limiting reactant) system. L_w: liquid water; H: hydrate; V: vapor (or gas); P: pressure.[2,4] Bold solid lines: L_w-H equilibrium; solid lines: L_w-G/V equilibrium; dashed lines: metastable L_w-G/V equilibrium; bold dashed lines: L_w-G/V-H equilibrium.

pressures including L_w-G/V and L_w-H equilibria concerning their reliability. Note that we consider the mole fraction of carbon dioxide/methane in the vapor/gas phase for performing thermodynamic consistency test for the latter phase. A similar method can be applied, of course, on the water content of the vapor/gas phase. It is expected that this study provides a better understanding of solubility in the carbon dioxide/methane + water system.

■ THERMODYNAMIC CONSISTENCY TEST

The thermodynamic relationship, which is frequently used to analyze thermodynamic consistency of experimental phase equilibrium data is the fundamental Gibbs−Duhem equation.[21−25] This equation, as presented in the literature, interrelates the activity coefficients/fugacities of all components in a given mixture. If this equation is not obeyed within the defined criteria, then the data are declared to be thermodynamically inconsistent. It means that this relation imposes a constraint on the activity coefficients/fugacities that is not satisfied by the experimental data.[21,22] This is due to various errors occurring during experimental works especially those dealing with high pressure and low temperature conditions.

The ways in which the Gibbs−Duhem equation[21−25] is arranged and applied to the experimental data have given origin to several "consistency test methods", most of them designed for low-pressure data. Among these are the slope test, the integral test, the differential test, and the tangent-intercept test.[21−26] Good reviews of these methods are given elsewhere.[24,25]

In the past decade, Valderrama and co-workers[26−30] have investigated the applications of numerical thermodynamic consistency methods to various systems including incomplete phase equilibrium data of high-pressure gas−liquid mixtures,[26] high pressure ternary mixtures of compressed gas and solid solutes,[27] high pressure gas−solid solubility data of binary mixtures,[28] vapor−liquid equilibrium data for mixtures containing ionic liquids,[29] and high pressure gas−liquid equilibrium data including both liquid and vapor phases.[30] Recently, Eslamimanesh et al.[31,32] have applied almost the same approach for performing the thermodynamic consistency test on significant systems encountered in oil and gas industries, for example, water content of methane in equilibrium with gas hydrate, liquid water, or ice[31] and sulfur content of hydrogen sulfide vapor.[32]

A method especially employed for determining thermodynamic consistency of high pressure gas−solid data by Valderrama and Alvarez,[26] which is based on rewriting the Gibbs−Duhem equation[21−25] in terms of fugacity coefficients,[33] has been used in this work. The consistency method employed here can be considered as a modeling procedure. This is because a thermodynamic model that can accurately represent the experimental data (i.e., the average deviations of the model results from experimental values are within the acceptable range according to the studied system and for a desired purpose) must be used to apply the consistency test. The fitting of the experimental data requires the calculation of some model parameters using a defined objective function that must be minimized.

As stated by Valderrama and Alvarez,[26] a suitable consistency test method to analyze high pressure data must fulfill 10 basic requirements:[26,31,32]

1. Uses the Gibbs−Duhem equation.[21−25]
2. Uses the fundamental equation of phase equilibrium.
3. Uses all of the experimental $P-T-z$ (pressure-temperature-solubility) data available for testing.
4. Does not necessarily require experimental data for the whole concentration range and be applicable for data in any range of concentration.
5. Be able to correlate the data within acceptable limits of deviations, deviations that must be evenly distributed.
6. Requires few additional calculated properties.
7. Be able to detect erroneous experimental points.
8. Makes appropriate use of necessary statistical parameters.
9. Be simple to be applied, with respect to the complexity of the problem to be solved.
10. Be able to conclude about consistency with regards to as defined criteria.

Expressions. The Gibbs−Duhem equation[21−25] for a binary homogeneous mixture at constant temperature can be written as:[23,24,26−32]

$$\left[\frac{v^{E}}{RT}\right]\mathrm{d}P = z_1\mathrm{d}(\ln \gamma_1) + z_2\mathrm{d}(\ln \gamma_2) \tag{1}$$

where v^E is the excess molar volume, T represents temperature, R stands for the universal gas constant, γ is the activity coefficient, z represents the solute mole fraction, P stands for pressure, and d is the derivative symbol. In this expression, subscripts 1 and 2 refer to components 1 and 2 in the present phases, respectively. Equation 1 can be written in terms of the fugacity coefficients as follows:[26−32]

$$\left[\frac{Z-1}{P}\right]\mathrm{d}P = z_1\mathrm{d}(\ln \varphi_1) + z_2\mathrm{d}(\ln \varphi_2) \tag{2}$$

where Z is the compressibility factor and φ stands for the fugacity coefficient.

This expression is rewritten in terms of the amount of carbon dioxide/methane in each phases. If these gases are considered as component 2 in the binary mixture of carbon dioxide/methane + water, the latter equation becomes:

$$\frac{1}{P}\frac{\mathrm{d}P}{\mathrm{d}z_2} = \frac{z_2}{(Z-1)}\frac{\mathrm{d}(\ln \varphi_2)}{\mathrm{d}z_2} + \frac{(1-z_2)}{(Z-1)}\frac{\mathrm{d}(\ln \varphi_1)}{\mathrm{d}z_2} \tag{3}$$

or in integral form as follows:

$$\int \frac{1}{Pz_2}\,\mathrm{d}P = \int \frac{1}{(Z-1)\varphi_2}\,\mathrm{d}\varphi_2 + \int \frac{(1-z_2)}{z_2(Z-1)\varphi_1}\,\mathrm{d}\varphi_1 \quad (4)$$

The properties φ_1, φ_2, and Z can be calculated using an equation of state and suitable mixing rules (thermodynamic model).

In eq 4, the left-hand side is designated by A_p and the right-hand side by A_φ, as follows:[26−32]

$$A_p = \int \frac{1}{Pz_2}\,\mathrm{d}P \quad (5)$$

$$A_\varphi = A_{\varphi 1} + A_{\varphi 2} \quad (6)$$

$$A_{\varphi 1} = \int \frac{(1-z_2)}{z_2(Z-1)\varphi_1}\,\mathrm{d}\varphi_1 \quad (7)$$

$$A_{\varphi 2} = \int \frac{1}{(Z-1)\varphi_2}\,\mathrm{d}\varphi_2 \quad (8)$$

Thus, if a set of data is considered to be consistent, A_P should be equal to A_φ within acceptable defined deviations. To set the margins of error, a percent area deviation ($\Delta A_i\%$) between experimental and calculated values is defined as:[26−32]

$$\Delta A_i\% = 100\left[\frac{A_{\varphi_i} - A_{p_i}}{A_{p_i}}\right] \quad (9)$$

where i refers to the data set number. The maximum values accepted for these deviations regarding the proposed systems are discussed later.

Liquid Water−Gas/Vapor Equilibrium. To evaluate the parameters for the consistency test in this region, that is, Z, φ_1, and φ_2, a previously tuned thermodynamic model[34−37] was applied. The general phase equilibrium criterion of equality of fugacities of each component throughout all phases was considered to model the phase behavior as follows:

$$f_i^{\mathrm{G/V}} = f_i^{\mathrm{L}} \quad (10)$$

where f is the fugacity, i refers to the ith component in the mixture, and superscripts G/V and L denote the gas/vapor and liquid phases, respectively. The Valderrama modification of the Patel and Teja equation of state (VPT EoS)[38] with nondensity-dependent (NDD) mixing rules[39] was used to calculate the compressibility factor, fugacity coefficients, and the mole fractions of components in liquid and vapor/gas phases.[34−37] The VPT EoS[38] with the NDD mixing rules[39] is given in the Appendix while the detailed description of the thermodynamic model can be found elsewhere.[1,34−37]

Liquid Water−Hydrate Equilibrium. The liquid water−hydrate equilibrium of a system is calculated by equating the fugacities of water in the liquid water phase, $f_{\mathrm{w}}^{\mathrm{L}}$, and in the hydrate phase, $f_{\mathrm{w}}^{\mathrm{H}}$:[2−4]

$$f_{\mathrm{w}}^{\mathrm{L}} = f_{\mathrm{w}}^{\mathrm{H}} \quad (11)$$

The fugacity of water in the hydrate phase, $f_{\mathrm{w}}^{\mathrm{H}}$, is related to the chemical potential difference of water in the filled and empty hydrate cage by the following expression:[2−4]

$$f_{\mathrm{w}}^{\mathrm{H}} = f_{\mathrm{w}}^{\mathrm{MT}} \exp\frac{\mu_{\mathrm{w}}^{\mathrm{H}} - \mu_{\mathrm{w}}^{\mathrm{MT}}}{RT} \quad (12)$$

where $f_{\mathrm{w}}^{\mathrm{MT}}$ is the fugacity of water in the hypothetical empty hydrate phase, $\mu_{\mathrm{w}}^{\mathrm{H}} - \mu_{\mathrm{w}}^{\mathrm{MT}}$ represents the chemical potential difference of water in the filled ($\mu_{\mathrm{w}}^{\mathrm{H}}$) and empty ($\mu_{\mathrm{w}}^{\mathrm{MT}}$) hydrate.

The solid solution theory of van der Waals−Platteeuw[40] can be employed for calculating $((\mu_{\mathrm{w}}^{\mathrm{H}} - \mu_{\mathrm{w}}^{\mathrm{MT}})/RT)$:[2−4]

$$\frac{\mu_{\mathrm{w}}^{\mathrm{H}} - \mu_{\mathrm{w}}^{\mathrm{MT}}}{RT} = -\sum_i \nu_i' \ln\Big(1 + \sum_j C_{ij} f_j\Big) = \sum_i \ln\Big(1 + \sum_j C_{ij} f_j\Big)^{-\nu_i'} \quad (13)$$

where ν_i' is the number of cavities of type i per water molecule in a unit hydrate cell,[2−4] C_{ij} stands for the Langmuir constant for hydrate former's interaction with each type cavity and f_j is the fugacity of hydrate former.[2−4]

The fugacity of water in the empty lattice can be expressed as:[2−4]

$$f_{\mathrm{w}}^{\mathrm{MT}} = P_{\mathrm{w}}^{\mathrm{MT}} \varphi_{\mathrm{w}}^{\mathrm{MT}} \exp\int_{P_{\mathrm{w}}^{\mathrm{MT}}}^{p} \frac{\nu_{\mathrm{w}}^{\mathrm{MT}}\,\mathrm{d}P}{RT} \quad (14)$$

where $P_{\mathrm{w}}^{\mathrm{MT}}$, $\varphi_{\mathrm{w}}^{\mathrm{MT}}$, and $\nu_{\mathrm{w}}^{\mathrm{MT}}$ are the vapor pressure of the empty hydrate lattice, the correction for the deviation of the saturated vapor of the pure (hypothetical) lattice from ideal behavior, and the partial molar volume of water in the empty hydrate,[2−4] respectively. The exponential term is a Poynting type correction.[2−4]

Equation 14 may be simplified by two assumptions: (1) that the hydrate partial molar volume is equal to the molar volume and is independent of pressure and (2) that $P_{\mathrm{w}}^{\mathrm{MT}}$ is relatively small (on the order of 10^{-3} MPa), so that $\varphi_{\mathrm{w}}^{\mathrm{MT}} = 1$.[2−4] Therefore,[2−4]

$$f_{\mathrm{w}}^{\mathrm{MT}} = P_{\mathrm{w}}^{\mathrm{MT}} \exp\frac{\nu_{\mathrm{w}}^{\mathrm{MT}}(P - P_{\mathrm{w}}^{\mathrm{MT}})}{RT} \quad (15)$$

Using the previous expressions, the following expression is obtained for the fugacity of water in the hydrate phase:[2,4]

$$f_{\mathrm{w}}^{\mathrm{H}} = P_{\mathrm{w}}^{\mathrm{MT}} \exp\left[\frac{\nu_{\mathrm{w}}^{\mathrm{MT}}(P - P_{\mathrm{w}}^{\mathrm{MT}})}{RT}\right] \cdot \left[(1 + C_{\mathrm{small}} f_{\mathrm{HF}}^{\mathrm{L}})^{-\nu_{\mathrm{small}}'}(1 + C_{\mathrm{large}} f_{\mathrm{HF}}^{\mathrm{L}})^{-\nu_{\mathrm{large}}'}\right] \quad (16)$$

where $f_{\mathrm{HF}}^{\mathrm{L}}$ is the fugacity of hydrocarbon hydrate former in the liquid water phase.[2,4]

The Poynting correction term can be ignored up to intermediate pressures, and therefore, eq 17 can be obtained for calculating fugacity of water in hydrate phase:[2,4]

$$f_{\mathrm{w}}^{\mathrm{H}} = P_{\mathrm{w}}^{\mathrm{MT}}\left[(1 + C_{\mathrm{small}} f_{\mathrm{HF}}^{\mathrm{L}})^{-\nu_{\mathrm{small}}'}(1 + C_{\mathrm{large}} f_{\mathrm{HF}}^{\mathrm{L}})^{-\nu_{\mathrm{large}}'}\right] \quad (17)$$

The fugacity of water in the liquid water phase can be expressed by:[2−4,21−23,25]

$$f_{\mathrm{w}}^{\mathrm{L}} = x_{\mathrm{w}}^{\mathrm{L}} \gamma_{\mathrm{w}}^{\mathrm{L}} P_{\mathrm{w}}^{\mathrm{sat}} \quad (18)$$

where $x_{\mathrm{w}}^{\mathrm{L}}$ and $\gamma_{\mathrm{w}}^{\mathrm{L}}$ are the water mole fraction and the activity coefficient of water in liquid water phase, respectively. In the intermediate pressure range, the liquid water is an incompressible fluid, the methane solubility is very small compared with unity; consequently the activity coefficient of water can be approximated to unity[2−4] (however, it is necessary to be careful, as it is not the case at high pressures where the nonideality of the liquid water phase and solubility become important[2−4]). Therefore, eq 19 can be satisfactorily written as below:[2,4]

$$f_{\mathrm{w}}^{\mathrm{L}} \cong P_{\mathrm{w}}^{\mathrm{sat}} \tag{19}$$

Using the above equations, the following expression is obtained for hydrocarbon hydrate former:[2,4]

$$P_{\mathrm{w}}^{\mathrm{sat}} = P_{\mathrm{w}}^{\mathrm{MT}}[(1 + C_{\mathrm{small}} f_{\mathrm{HC}}^{\mathrm{L}})^{-\nu'_{\mathrm{small}}}(1 + C_{\mathrm{large}} f_{\mathrm{HC}}^{\mathrm{L}})^{-\nu'_{\mathrm{large}}}] \tag{20}$$

or

$$1 - \left(\frac{P_{\mathrm{w}}^{\mathrm{MT}}}{P_{\mathrm{w}}^{\mathrm{sat}}}\right)[(1 + C_{\mathrm{small}} f_{\mathrm{HC}}^{\mathrm{L}})^{-\nu'_{\mathrm{small}}}(1 + C_{\mathrm{large}} f_{\mathrm{HC}}^{\mathrm{L}})^{-\nu'_{\mathrm{large}}}] = 0 \tag{21}$$

The subscript HC represents pure hydrocarbon hydrate former (methane). The fugacity of hydrocarbon hydrate former in the liquid water phase up to intermediate pressures can be calculated using the following equation:[2,4]

$$f_{\mathrm{HC}}^{\mathrm{L}} = x_{\mathrm{HC}}^{\mathrm{L}} H_{\mathrm{HC-w}} \tag{22}$$

where $H_{\mathrm{HC-w}}$ represents Henry's constant for hydrocarbon hydrate former—water system. Therefore, the following final expression is obtained for estimating the solubility of pure hydrocarbon hydrate former in liquid water phase being in equilibrium with gas hydrates:[2,4]

$$1 - \left(\frac{P_{\mathrm{w}}^{\mathrm{MT}}}{P_{\mathrm{w}}^{\mathrm{sat}}}\right)[(1 + C_{\mathrm{small}} x_{\mathrm{HC}}^{\mathrm{L}} H_{\mathrm{HC-w}})^{-\nu'_{\mathrm{small}}}$$

$$(1 + C_{\mathrm{large}} x_{\mathrm{HC}}^{\mathrm{L}} H_{\mathrm{HC-w}})^{-\nu'_{\mathrm{large}}}] = 0 \tag{23a}$$

Equation 23a allows easy calculation of the solubility of pure hydrocarbon hydrate former in the liquid water being in equilibrium with gas hydrates. Its main advantages are the availability of necessary input data and the simplicity of the calculations that can be done even in Microsoft Excel spreadsheets (without requirement of long programming codes).[2,4] Furthermore, as can be seen in eq 23a, almost all terms are temperature-dependent while not pressure-dependent, indicating the solubility of pure hydrocarbon hydrate former in liquid water phase being in equilibrium with gas hydrate is a strong function of temperature and only a weak function of pressure. For the CO_2 (and other highly soluble gases like H_2S) and water system, the solubility of CO_2 in the water phase cannot be ignored, and consequently, the water activity cannot be set to unity. Taking into account the CO_2 solubility in the water phase and also the water activity, the following equation can be derived:[2,5]

$$1 - \left[\frac{P_{\mathrm{w}}^{\mathrm{MT}}}{(1 - x_{\mathrm{CO_2}}^{\mathrm{L}})\gamma_{\mathrm{w}}^{\mathrm{L}} P_{\mathrm{w}}^{\mathrm{sat}}}\right][(1 + C_{\mathrm{small}} x_{\mathrm{CO_2}}^{\mathrm{L}} H_{\mathrm{CO_2-w}})^{-\nu'_{\mathrm{small}}}$$

$$(1 + C_{\mathrm{large}} x_{\mathrm{CO_2}}^{\mathrm{L}} H_{\mathrm{CO_2-w}})^{-\nu'_{\mathrm{large}}}] = 0 \tag{23b}$$

Table 1. Constants *a* to *d* in Equations 26 and 27[2,4,42]

	a	*b*	*c*	*d*
hydrate former	K·MPa^{-1}	K·MPa^{-1}	K·MPa^{-1}	K·MPa^{-1}
methane	0.0037237	2708.8	0.018373	2737.9
CO_2	0.0011978	2860.5	0.008507	3277.9

Table 2. Constants *A* to *D* in Equation 29[2,4,46]

hydrate former	A	B/K	$\bar{C}$/K^{-1}	D/K^{-1}	T_{min}/K	T_{max}/K
methane	147.788	−5768.3	−52.2952	0.018616	273.15	373.15
CO_2	21.6215	−1499.8	−5.64947	0.0002062	273.15	373.15

Table 3. Critical Properties (T_c, P_c, v_c) and Acentric Factor (ω) of Investigated Pure Compounds Used in the VPT-EoS[35]

	P_c	T_c	v_c	
compound	MPa	K	m^3·kg·mol^{-1}	ω
water	22.064	647.13	0.056	0.3443
methane	4.599	190.564	0.0992	0.0114
carbon dioxide	7.377	304.13	0.094	0.2239

Model Parameters. In eqs 23a and 23b, the following values of ν'_i for structure-I hydrates can be used:[2−4,41]

$$\nu'_{\mathrm{small}} = \frac{1}{23} \tag{24a}$$

$$\nu'_{\mathrm{large}} = \frac{3}{23} \tag{24b}$$

and for structure II:

$$\nu'_{\mathrm{small}} = \frac{2}{17} \tag{25a}$$

$$\nu'_{\mathrm{large}} = \frac{1}{17} \tag{25b}$$

Note that carbon dioxide and methane form structure-I clathrate hydrates. The Langmuir constants accounting for the interaction between the hydrate former and water molecules in the cavities were reported by Parrish and Prausnitz[42] for a range of temperatures and hydrate formers.[2,4] However, the integration procedure was followed in obtaining the Langmuir constants for wider temperatures using the Kihara[43] potential function with a spherical core according to the study by McKoy and Sinanoĝlu.[44] In this work, the Langmuir constants for the hydrate former's interaction with each type cavity have been determined using the equations of Parrish and Prausnitz:[42]

For small cavity:

$$C_{\mathrm{small}} = \frac{a}{T}\exp\left(\frac{b}{T}\right) \tag{26}$$

For large cavity:

$$C_{\mathrm{large}} = \frac{c}{T}\exp\left(\frac{d}{T}\right) \tag{27}$$

where T is in K and C has units of reciprocal MPa. Constants a to d are reported in Table 1.[2,42]

The concept in eq 14 of universal empty hydrate vapor pressure for each structure prompted Dharmawardhana et al.[45]

Table 4. Experimental Data Ranges Used for Consistency Tests in This Work

				range of experimental data			
system	set no.	T/K	N[a]	P/MPa	$x_2^{\mathrm{exp}} \cdot 10^6$/mole fraction	$y_2^{\mathrm{exp}} \cdot 10^5$/mole fraction	ref[b]
Carbon Dioxide							
L_w-G/V-E[c]	1	323.15	7	6.820—17.680	16510—22620	99661—99357	51
	2	298.20	3	3.630—6.420	18300—24700	99860—99890	52
	3	323.20	7	7.080—14.110	17600—21700	99660—99390	53
	4	333.20	10	4.050—14.110	9600—20800	99340—99220	53
	5	353.10	9	4.050—13.100	8000—18400	98570—99000	53
	6	308.80	7	1.166—7.957	8000—50600	89900—99000	54
	7	373.15	6	0.600—2.307	980—4140	84500—95500	55
	8	393.15	5	0.599—2.848	1810—4280	84000—92600	55
	9	413.15	3	2.010—3.247	2580—430	80000—87200	55
	10	323.15	7	6.820—17.680	16510—22620	99357—99661	56
	11	383.15	15	10.000—150.000	14000—40000	96969—97399	57
	12	423.15	15	10.000—150.000	13500—48000	75200—88000	57
	13	473.15	14	20.000—150.000	13000—72000	69000—82000	57
L_w-H-E[d]	14	274.05	2	4.200—5.000	15600—16300		58
	15	280.50	8	4.990—14.200	25600—26000		59
	16	278.50	4	6.100—10.410	22100—23500		59
	17	279.50	5	6.100—10.440	26200—24100		59
Methane							
L_w-G-E	1	298.15	10	2.351—44.402	497—4170	-[e]	60
	2	310.93	12	2.275—68.223	440—4650	-	60
	3	344.26	9	6.501—68.017	340—4240	-	60
	4	377.59	13	2.296—68.086	323—4510	-	60
	5	310.93	9	3.516—2.965	64—588	-	61
	6	327.59	7	0.779—3.592	128—564	-	61
	7	344.26	7	0.772—3.268	105—477	-	61
	8	360.93	9	0.786—3.702	126—57	-	61
	9	298.15	9	1.103—5.171	214—1130	-	61
	10	303.15	8	0.317—3.605	60—764	-	61
	11	274.35	8	0.567—2.806	258—1142	-	61
	12	285.65	5	2.331—9.082	656—2000	-	61
	13	283.37	4	1.765—7.046	562—1850	-	62
	14	275.11	4	0.973—2.820	399—1061	-	63
	15	283.13	4	1.039—5.977	329—1496	-	63
	16	313.11	4	1.025—17.998	204—2325		63
	17	313.15	5	2.500—12.500	490—1870	99697—99907	64
	18	338.15	5	2.500—12.500	400—1620	99017—99702	64
	19	473.15	6	30.000—150.000	5000—13000	81100—89000	65
	20	423.15	6	9.807—98.066	100—5600	94000—98500	66
	21	473.15	5	19.613—98.066	3800—10400	81000—96300	66
	22	298.15	5	2.500—12.500	590—2210	99746—99941	66
L_w-H-E	23	278.10	7	5.790—19.350	960—1140		67
	24	278.20	4	8.890—13.760	1040—1060		67
	25	273.10	8	4.980—14.810	765—775		67
	26	274.15	4	6.000—20.000	1106—1264		68
	27	278.15	4	6.000—20.000	1322—1452		68
	28	282.15	3	10.000—20.000	1583—1687		68
	29	286.15	2	15.000—20.000	1799—1826		68
	30	278.10	7	5.790—19.350	960—1140		69
	31	278.20	4	8.890—13.760	1040—1060		69
	32	273.10	8	4.980—14.810	775—765		69

[a] Number of experimental data points. [b] Reference of experimental data. [c] Liquid water—gas/vapor equilibria. [d] Liquid water—hydrate equilibria. [e] Not available.

to calculate the P_w^{MT} from a number of simple hydrate three-phase ice—vapor—hydrate equilibrium. By equating the fugacity of water in the hydrate phase to that of pure ice at the three-phase line, Dharmawardhana et al.[45] obtained the following equation for the vapor pressure of the empty hydrate structure I:[2−4]

$$P_w^{\mathrm{MT}} = 0.1 \exp\left(17.440 - \frac{6003.9}{T}\right) \qquad (28a)$$

and for structure II:

$$P_w^{\mathrm{MT}} = 0.1 \exp\left(17.332 - \frac{6017.6}{T}\right) \qquad (28b)$$

where P_w^{MT} is in MPa and T is in K. It should be mentioned that the nonideality of water vapor pressure of the empty hydrate at

Table 5. Typical Calculated/Predicted Results of Solubilities in the Carbon Dioxide + Water (mole fraction)

set no.[a]	T/K	P/MPa	$x_2^{\text{exp}}\cdot 10^2$/mole fraction	$x_2^{\text{calc/pred}}\cdot 10^2$/mole fraction	$y_2^{\text{exp}}\cdot 10$/mole fraction	$y_2^{\text{calc/pred}}\cdot 10$/mole fraction	ARD[b] %/$x_2^{\text{calc/pred}}$	ARD [c]%/$y_2^{\text{calc/pred}}$
1	323.15	6.82	1.651	1.711	9.9661	9.9650	3.7	0.01
		7.53	1.750	1.812	9.9655	9.9651	3.5	0.00
		8.72	1.768	1.948	9.9636	9.9636	10.2	0.00
		10.13	2.081	2.061	9.9564	9.9578	1.0	0.01
		12.21	2.096	2.162	9.9457	9.9480	3.2	0.02
		14.75	2.215	2.249	9.9392	9.9413	1.5	0.02
		17.68	2.262	2.329	9.9357	9.9366	3.0	0.01
2	298.2	3.63	1.830	1.754	9.986	9.9871	4.2	0.01
		6.41	2.440	2.468	9.986	9.9879	1.1	0.02
		6.42	2.470	2.469	9.989	9.9878	0.0	0.01
3	323.2	4.05	1.090	1.183	9.954	9.9566	8.6	0.03
		5.06	1.370	1.401	9.964	9.9615	2.3	0.03
		6.06	1.610	1.588	9.963	9.9641	1.4	0.01
		7.08	1.760	1.749	9.966	9.9651	0.7	0.01
		8.08	1.900	1.878	9.966	9.9647	1.1	0.01
		9.09	2.000	1.982	9.959	9.9625	0.9	0.04
		10.09	2.050	2.058	9.955	9.9580	0.4	0.03
		11.1	2.100	2.113	9.95	9.9526	0.6	0.03
		12.1	2.140	2.157	9.945	9.9483	0.8	0.03
		14.11	2.170	2.228	9.939	9.9426	2.7	0.04
4	333.2	4.05	0.960	1.011	9.934	9.9318	5.3	0.02
		5.06	1.210	1.205	9.945	9.9402	0.4	0.05
		6.06	1.380	1.376	9.945	9.9450	0.3	0.00
		7.08	1.570	1.527	9.949	9.9476	2.7	0.01
		8.08	1.660	1.655	9.95	9.9485	0.3	0.02
		9.09	1.790	1.765	9.953	9.9479	1.4	0.05
		10.09	1.860	1.854	9.951	9.9459	0.3	0.05
		11.1	1.950	1.928	9.947	9.9424	1.1	0.05
		12.1	2.010	1.986	9.942	9.9381	1.2	0.04
		14.11	2.080	2.078	9.922	9.9301	0.1	0.08
5	353.1	4.05	0.800	0.776	9.857	9.8458	3.0	0.11
		6.06	1.140	1.079	9.891	9.8799	5.3	0.11
		7.08	1.280	1.213	9.896	9.8883	5.2	0.08
		8.08	1.400	1.331	9.903	9.8935	4.9	0.10
		9.09	1.510	1.438	9.908	9.8964	4.8	0.12
		10.09	1.600	1.533	9.907	9.8975	4.2	0.10
		11.1	1.720	1.617	9.91	9.8971	6.0	0.13
		12.1	1.760	1.691	9.904	9.8956	3.9	0.08
		13.1	1.840	1.756	9.9	9.8931	4.5	0.07

[a] Refer to Table 4 for observing the data set number. [b] ARD = $100\cdot((|x_2^{\text{calc/pred}} - x_2^{\text{exp}}|)/x_2^{\text{exp}})$. [c] ARD = $100\cdot((|y_2^{\text{calc/pred}} - y_2^{\text{exp}}|)/y_2^{\text{exp}})$. (For better observation of the deviations of the calculated/predicted results from experimental values in the gas/vapor phase, they are shown with three digits).

saturation seems to be negligible due to the small quantity (typically, 10^{-3} to 10^{-5} MPa).

The following values for Henry's constant of hydrate former and water can be used:[2,4,46]

$$H_{\text{g,w}}(T) = (10^{A + B/T + \overline{C}\log(T) + DT})\cdot 0.1 \qquad (29)$$

where T and $H_{\text{g,w}}(T)$ are in K and MPa, respectively. Constants A, B, $\overline{C}$, and D are given in Table 2.

The water vapor pressure can be obtained using the following expression:[2,47]

$$P_{\text{w}}^{\text{sat}} = 10^{-6}\exp(73.649 - 7258.2/T - 7.3037\ln(T) + 4.1653\cdot 10^{-6}T^2) \qquad (30)$$

where T and $P_{\text{w}}^{\text{sat}}$ are, respectively, in Kelvin and MPa. Finally, Table 3 shows the critical properties and acentric factors of the pure compounds used in the VPT EoS.[35,38] The interaction parameters of the NDD mixing rules[39] are given elsewhere.[34]

Methodology. The following algorithm was applied for the thermodynamic consistency test:[26,31,32]

1 Determine A_p from eq 5 using the experimental $P-T-z$ data. Use a numerical integration for this purpose. In this work, Simpson's 3/8 rule[48] was used. Valderrama and Alvarez[26] have demonstrated that the deviations between the calculated values of the integrals by the simple trapezoidal integration rule and a fitted polynomial function are below 2 %. Therefore, a simple numerical integration method, for example, trapezoidal rule can be applied for the cases that there are only two available experimental data points.

2 Evaluate A_φ by eqs 6 to 8 using the obtained values for φ_2 and Z from the thermodynamic model[34−37] for the proposed system and z_2 from experimental data.

3 For every set of the experimental data, determine an absolute percent area deviation (ΔA_i %) between experimental ($A_{pi.}$) and calculated values ($A_{\varphi i}$) as follows, as mentioned before:

$$\Delta A_i\% = 100\left[\frac{A_{\varphi_i} - A_{pi}}{A_{pi}}\right] \qquad (31)$$

where i refers to the data set number.

Consistency Criteria. First and perhaps most important is the fact that the thermodynamic model should lead the average absolute

Table 6. Typical Calculated/Predicted Results of Solubilities in the Methane + Water System (mole fraction)

set no.[a]	T/K	P/MPa	$x_2^{exp} \cdot 10^4$/ mole fraction	$x_2^{calc/pred} \cdot 10^4$/ mole fraction	$y_2^{exp} \cdot 10$/ mole fraction	$y_2^{calc/pred} \cdot 10$/ mole fraction	ARD %/$x_2^{calc/pred}$	ARD %/$y_2^{calc/pred}$
1	298.15	2.351	4.97	5.43	-[b]	9.9852	9.2	
		3.165	7.17	7.11	-	9.9886	0.8	
		4.544	10.00	9.77	-	9.9916	2.3	
		6.44	13.17	13.04	-	9.9937	1	
		8.894	16.78	16.72	-	9.9949	0.3	
		13.307	22.35	22.09	-	9.9960	1.2	
		17.202	25.85	25.87	-	9.9965	0.1	
		24.235	31.10	31.29	-	9.9969	0.6	
		33.164	36.60	36.67	-	9.9972	0.2	
		44.402	41.70	42.14	-	9.9975	1.1	
2	310.93	2.275	4.40	4.53	-	9.9687	3	
		3.289	6.19	6.37	-	9.9776	2.9	
		4.578	8.39	8.55	-	9.9831	1.9	
		6.55	11.23	11.57	-	9.9874	3.1	
		8.756	14.40	14.58	-	9.9898	1.2	
		13.1	18.90	19.54	-	9.9921	3.4	
		17.754	22.90	23.81	-	9.9933	4	
		24.373	27.60	28.70	-	9.9942	4	
		33.853	33.30	34.24	-	9.9949	2.8	
		44.988	39.10	39.50	-	9.9954	1	
		54.262	41.70	43.23	-	9.9957	3.7	
		68.224	46.50	48.09	-	9.9960	3.4	
3	344.26	2.282	3.40	3.55	-	9.8463	4.4	
		3.22	4.70	4.92	-	9.8882	4.8	
		4.544	6.32	6.77	-	9.9178	7.1	
		6.502	9.09	9.30	-	9.9394	2.4	
		9.101	11.83	12.36	-	9.9536	4.4	
		12.962	15.00	16.33	-	9.9641	8.9	
		17.616	19.24	20.41	-	9.9705	6.1	
		24.373	23.85	25.35	-	9.9754	6.3	
		33.957	27.70	31.03	-	9.9792	12	
		44.988	34.20	36.35	-	9.9817	6.3	
		56.675	37.50	41.07	-	9.9835	9.5	
		68.017	42.40	45.03	-	9.9847	6.2	
4	377.59	2.296	3.23	3.21	-	9.4474	0.6	
		3.213	4.32	4.49	-	9.5966	3.9	
		3.227	4.72	4.51	-	9.5982	4.5	
		4.495	6.11	6.21	-	9.7032	1.6	
		6.516	8.86	8.76	-	9.7859	1.1	
		9.032	11.88	11.70	-	9.8370	1.5	
		13.1	15.60	15.96	-	9.8779	2.3	
		17.478	19.80	20.00	-	9.9005	1	
		24.614	25.10	25.63	-	9.9202	2.1	
		34.232	31.40	31.89	-	9.9341	1.6	
		44.988	36.10	37.67	-	9.9430	4.3	
		56.468	40.80	42.85	-	9.9493	5	
		68.086	45.10	47.35	-	9.9538	5	
19	473.15	20	50.00	35.00	8.110	8.8611	30	9.26
		30	60.00	49.06	8.460	9.1541	18.2	8.20
		40	70.00	60.73	8.690	9.3067	13.3	7.10
		50	80.00	70.54	8.850	9.4025	11.8	6.24
		70	90.00	86.05	8.880	9.5190	4.4	7.20
		100	110.00	102.35	8.900	9.6153	7	8.04
		150	130.00	118.62	8.900	9.6994	8.8	8.98
20	423.15	9.807	10.00	13.87	9.400	9.3952	38.7	0.05
		19.613	18.00	25.24	9.630	9.6487	40.2	0.19
		39.227	30.00	41.87	9.780	9.7791	39.6	0.01
		58.84	46.00	53.75	9.830	9.8265	16.8	0.04
		78.453	56.00	62.79	9.835	9.8527	12.1	0.18
		98.067	56.00	69.91	9.850	9.8699	24.8	0.20
21	473.15	19.613	38.00	34.39	8.915	8.8440	9.5	0.80
		39.227	67.00	59.90	9.350	9.2975	10.6	0.56
		58.84	87.00	77.98	9.480	9.4625	10.4	0.18
		78.453	10.00	91.35	9.545	9.5525	8.7	0.08
		98.067	10.40	101.48	9.630	9.6106	2.4	0.20

[a] Refer to Table 1 for observing the data set number. [b] Not available.

deviations of the results from experimental values to be within the acceptable range. Generally, the accepted deviations (ARDs) in liquid and gas/vapor phase mole fraction predictions (defined by the following equation) lie between (0 and 20) % for the liquid water−gas/vapor region and (0 and 30) % for liquid water−hydrate region:[2,4,26]

$$\mathrm{ARD}\% = 100\frac{|z_i^{\mathrm{calc/pred}} - z_i^{\mathrm{exp}}|}{z_i^{\mathrm{exp}}} \tag{32}$$

where superscripts calc/pred and exp refer to calculated/predicted and experimental values, respectively.

It is shown that that the average absolute deviations (ARDs) % of the model results used in this work are less than 20 % for the experimental data points in the L_w-G/V region and less than 30 % for those in the L_w-H region. Therefore, the model is completely acceptable for a thermodynamic consistency test of the L_w-G/V region (except for one data set) and generally acceptable for the L_w-H region after eliminating the points corresponding to weak predictions.

For determination of the acceptable percentages of the two evaluated area deviations from each other, the error propagation was performed on the existing experimental data. This was done using the general equation of error propagation,[49,50] considering the temperature and mole fraction of carbon dioxide/methane in either liquid or vapor/gas phases as the independent measured variables.[26] The calculated individual area (A_φ) is the dependent variable of interest. The error in the calculated areas, E_A, and the percent error, E_A %, are calculated as follows:[27,30,31]

$$E_A = \left[\frac{\partial A_{\varphi j}}{\partial T}\right]\Delta T + \left[\frac{\partial A_{\varphi j}}{\partial z}\right]\Delta z \tag{33}$$

$$E_A\,\% = 100\left[\left|\frac{E_A}{A_{\varphi j}}\right|\right] \tag{34}$$

where subscript j refers to jth calculated area. We assumed maximum uncertainties of 0.1 K for the experimental temperature and 10 % for the experimental solubility data outside of hydrate region while 20 % regarding the data inside of hydrate formation region. However, these uncertainties depend on the method of experimental measurements. The maximum acceptable errors are more dependent on the uncertainty of solubility measurements, and one can also neglect the first right-hand side term of eq 33. But the uncertainty for the measurements of solubility of carbon dioxide/methane with water, especially in hydrate formation region, is high, and that is why we imperatively need to perform the thermodynamic consistency test of such data.

Because of the fact that analytical derivatives are not so easy regarding the expression of the VPT EoS[38] with NDD mixing rules[39] and the applied equations for hydrate formation region, the partial derivatives of the two preceding equations have been evaluated using the central finite difference[48] method. It results in the ΔA_i % between (0 to 40) % for the data related to outside of hydrate formation region and (0 to 50) % for the data within the hydrate formation region. Therefore, the range (0 to 40) % is established as the maximum acceptable error for the areas ($[A_i]$) (below the curves calculated from the numerical integration) related to outside of hydrate formation region and (0 to 50) % for the corresponding areas related to the data of inside the hydrate formation region. The high uncertainty in measurements of the mutual solubilities of the investigated gases with water and also low concentrations of these components in liquid phase in hydrate forming conditions, contribute this wide range of acceptable area deviations for the data to be thermodynamically consistent.

Regarding these facts, the thermodynamic consistency test criteria are applied through the following instructions:[26−31]

1. Make sure the percentage Δz_2 is not outside of the margin of error: (0 to 20) % for the L_w-G/V region and (0 to 30) % for L_w-H. If it is outside the margin of error, change the thermodynamic model, or eliminate the weak calculations/predictions until the absolute deviations of the results from experimental values would be within the acceptable range.
2. If the model represents the data within the acceptable error ranges of the solubility results and the area test is fulfilled for all points in the data set, the proposed model is reliable, and the data seem to be thermodynamically consistent.
3. In the case that the model represents the data acceptably and the area test is not accomplished for most of the data set (more than 75 % of the areas), the applied model is reliable, but the experimental data are suspected to be thermodynamically inconsistent.
4. In the case that the model acceptably represents the data and some of the area deviations (equal or less than 25 % of the areas) are outside the error range (0 to 40) % for the data of outside hydrate formation region and (0 to 50) % for the data regarding the inside of this region, the applied method suspects the experimental values as being not fully consistent.

■ RESULTS AND DISCUSSION

Forty-nine (isothermal) experimental data sets have been investigated for consistency test in this work. Table 4 summarizes the ranges of the data along with the references. These data contain various pressures, temperatures, and solubility values available in the literature.

As can be observed in Tables 5 and 6, the thermodynamic models used in this work generally result in reliable predictions/representations of mutual solubilities/solubilities for investigated equilibrium conditions. All of the results of calculations of the solubilities are presented as Supporting Information.

Table 7 reports the typical results of the thermodynamic consistency test for solubility of carbon dioxide in water. The typical results of the consistency test for the experimental data of the carbon dioxide + water gas phase are reported in Table 8. All of the test results are presented as Supporting Information. These results show that about 47 % of the investigated experimental data of solubility of carbon dioxide in water seem to be thermodynamically consistent; meanwhile this percentage is around 53 % for inconsistent data and 0 % for not fully consistent data. These percentages are about 31 %, 46 %, and 23 % for the data of concentrations of carbon dioxide in the gas phase, respectively.

Table 9 shows the typical results of the thermodynamic consistency test for the data of solubility of methane in water (refer to the Supporting Information for reviewing the complete test results). It is found out from these results that around 16 % of the investigated experimental data of solubilities of methane in water seem to be thermodynamically consistent while this percentage is around 78 % for inconsistent data and about 6 % for not fully consistent data. It is inferred that the area deviations of these sets of data are higher than those ones for solubility of carbon dioxide. This is mainly because of lower solubility of

Table 7. Typical Detailed Results of Thermodynamic Consistency Test on the Experimental Data of the Solubility of Carbon Dioxide in Water Investigated in This Work

set no.[a]	T/K	P/MPa	Z	φ_1^{L}	φ_2^{L}	A_p	A_φ	ΔA %	test result[b]
1	323.15	6.82	0.0495	0.013	50.074	48.478	53.189	9.7	TC
		7.53	0.0547	0.011	43.789				
		8.72	0.0634	0.010	36.387				
		10.13	0.0737	0.008	30.740				
		12.21	0.0889	0.007	25.601				
		14.75	0.1075	0.005	21.631				
		17.68	0.1288	0.004	18.594				
2	298.2	3.63	0.0281	0.007	67.203	14.55	22.694	56	TI
		6.41	0.0499	0.004	28.869				
		6.42	0.0500	0.004	28.813				
3	323.2	7.08	0.0514	0.012	47.611	30.702	38.172	24.3	TC
		8.08	0.0587	0.011	40.013				
		9.09	0.0661	0.009	34.679				
		10.09	0.0734	0.008	30.896				
		11.1	0.0808	0.007	28.049				
		12.1	0.0881	0.007	25.837				
		14.11	0.1028	0.006	22.498				
4	333.2	4.05	0.0286	0.127	68.918	87.855	399.217	354.4	TI
		5.06	0.0358	0.111	55.786				
		6.06	0.0429	0.094	47.329				
		7.08	0.0502	0.022	56.219				
		8.08	0.0573	0.018	47.604				
		9.09	0.0645	0.015	41.243				
		10.09	0.0716	0.013	36.568				
		11.1	0.0788	0.012	32.982				
		12.1	0.0860	0.010	30.216				
		14.11	0.1003	0.009	26.142				
5	353.1	4.05	0.0273	0.132	92.985	73.389	132.686	80.8	TI
		6.06	0.0410	0.108	62.937				
		7.08	0.0479	0.095	54.484				
		8.08	0.0548	0.082	48.478				
		9.09	0.0616	0.067	44.099				
		10.09	0.0685	0.050	41.486				
		11.1	0.0753	0.034	40.166				
		12.1	0.0822	0.027	37.753				
		13.1	0.0890	0.023	35.280				

[a] Refer to Table 4 for observing the data set number. [b] TI: thermodynamically inconsistent data. TC: thermodynamically consistent data. Refer to the Supporting Information for observing all of the detailed consistency test results.

Table 8. Typical Detailed Results of Thermodynamic Consistency Test on the Experimental Data of the Concentration of Carbon Dioxide in Gas Phase Investigated in This Work

set no.[a]	T/K	P/MPa	Z	φ_1^{G}	φ_2^{G}	A_p	A_φ	ΔA %	test result
1	323.15	6.82	0.6612	3.727	0.860	0.932	1.145	22.9	TC
		7.53	0.6152	3.246	0.796				
		8.72	0.5290	2.581	0.711				
		10.13	0.4221	1.809	0.636				
		12.21	0.3632	1.173	0.556				
		14.75	0.3724	0.846	0.489				
		17.68	0.4032	0.654	0.436				
3	323.2	7.08	0.6451	3.559	0.835	0.617	0.838	35.9	TI
		8.08	0.5773	3.034	0.754				
		9.09	0.5005	2.187	0.690				
		10.09	0.4253	1.765	0.638				
		11.1	0.3795	1.424	0.596				
		12.1	0.3642	1.173	0.560				
		14.11	0.3677	0.888	0.504				
4	333.2	4.05	0.8354	18.992	0.701	1.308	0.756	42.2	TI
		5.06	0.7907	19.859	0.676				
		6.06	0.7444	16.825	0.655				
		7.08	0.6948	14.206	0.641				
		8.08	0.6437	3.494	0.792				
		9.09	0.5899	3.135	0.732				
		10.09	0.5364	2.609	0.682				
		11.1	0.4875	2.129	0.639				
		12.1	0.4519	1.744	0.604				
		14.11	0.4232	1.073	0.547				
5	353.1	4.05	0.8671	9.163	0.733	0.978	0.552	43.5	NFC[b]
		6.06	0.7990	9.777	0.688				
		7.08	0.7639	9.012	0.668				
		8.08	0.7293	8.319	0.652				
		9.09	0.6946	7.229	0.641				
		10.09	0.6610	5.325	0.642				
		11.1	0.6287	3.674	0.656				
		12.1	0.5996	2.718	0.645				
		13.1	0.5744	2.216	0.626				
6	308.8	1.17	0.9418	1.684	0.767	0.613	0.311	49.3	TI
		2.27	0.8836	2.599	0.725				
		3.8	0.7947	23.238	0.674				
		5.14	0.7053	69.842	0.641				
		5.26	0.6964	7.648	0.640				
		6.19	0.6210	0.670	0.828				
		7.96	0.3678	0.512	0.672				

[a] Refer to Table 4 for observing the data set number. [b] Not fully consistent data. Refer to the Supporting Information for observing all of the detailed consistency test results.

methane in water and therefore the expected difficulties of experimental measurements for such systems.[1,63] The typical results of the consistency test for the experimental data of the methane + water gas phase are reported in Table 10 (refer to the Supporting Information for reviewing the complete test results). The percentages of consistent, inconsistent, and not fully consistent data seem to be around 0 %, 50 %, and 50 %, respectively, regarding these data. As for the not fully consistent data, the eliminated data points and the calculation results are available upon request to the authors. Moreover, for a better understanding of the evaluated integrals in eqs 5 to 8, typical sketches have been presented in Figures 2 to 4 regarding the data set 3 for solubility of methane in water.

It is obvious that using more developed experimental apparatus results in accurate measurements of solubilities of carbon dioxide/methane in water especially for equilibrium with gas hydrates, whereas these types of measurements were not studied almost 15 years ago. Additionally, the results of such a test introduce a procedure to select the experimental data by which a thermodynamic model is supposed to be tuned and optimal values of the model parameters are supposed to be obtained. Thermodynamically inconsistent data (sometimes not fully consistent data) used for tuning of the models may bring about inaccurate predictions of the model in further applications, and the cause of such deviations may not be easily figured out.

Another element to consider is that the data, on which the presented thermodynamic consistency test is applied, should be reported as isotherms because the main assumption in the development of eqs 1 to 8 is similar to that assumed in developing the original Gibbs−Duhem equation[21−25] at constant temperature. This fact assigns some limitations to choose the experimental data sets for consistency test using the applied method especially for scarce data of solubilities of gases in water in equilibrium with gas hydrates. One way of solving this problem of few data may be generating more data in a statistical form using statistical software. The generated data are treated as

Table 9. Typical Detailed Results of Thermodynamic Consistency Test on the Experimental Data of the Solubility of Methane in Water Investigated in This Work

set no.[a]	T/K	P/MPa	Z	φ_1^L	φ_2^L	A_p	A_φ	ΔA %	test result
22	298.15	2.5	0.0191	0.151	1359.345	1214.417	868.403	28.5	TC
		5	0.0383	0.112	721.499				
		7.5	0.0574	0.081	513.449				
		10	0.0766	0.057	413.267				
		12.5	0.0957	0.039	355.881				
1	298.15	2.351	0.0180	0.154	1440.584	6114.053	3365.225	45	TI
		3.165	0.0242	0.140	1090.400				
		4.544	0.0348	0.119	785.027				
		6.44	0.0493	0.093	581.289				
		8.894	0.0681	0.066	450.092				
		13.307	0.1019	0.035	342.255				
		17.202	0.1317	0.021	294.139				
		24.235	0.1855	0.011	243.281				
		33.164	0.2537	0.007	208.795				
		44.402	0.3395	0.005	187.384				
2	310.93	2.275	0.0168	0.159	1734.786	8774.705	4213.965	52	TI
		3.289	0.0243	0.144	1224.711				
		4.578	0.0339	0.126	904.786				
		6.55	0.0485	0.102	660.920				
		8.756	0.0648	0.079	521.156				
		13.1	0.0969	0.047	388.367				
		17.754	0.1313	0.029	320.724				
		24.373	0.1802	0.017	268.099				
		33.853	0.2502	0.010	228.279				
		44.988	0.3323	0.007	205.213				
		54.262	0.4005	0.006	195.896				
		68.224	0.5031	0.005	191.361				
19	473.15	19.613	0.1117	0.072	266.396	202.007	30.2	85	TI
		39.227	0.2217	0.076	155.805				
		58.84	0.3301	0.068	128.816				
		78.453	0.4369	0.062	120.899				
		98.067	0.5423	0.059	121.054				
26	274.15	6	0.0493	0.000	467.647	1052.33	1434.4	36.3	TC
		10	0.0821	0.000	280.588				
		15	0.1231	0.000	187.059				
		20	0.1640	0.000	140.294				

[a] Refer to Table 4 for observing the data set number. Refer to the Supporting Information for observing all of the detailed consistency test results.

Table 10. Typical Detailed Results of Thermodynamic Consistency Test on the Experimental Data of the Concentration of Methane in the Gas Phase Investigated in This Work

set no.[a]	T/K	P/MPa	Z	φ_1^G	φ_2^G	A_p	A_φ	ΔA %	test result
22	298.15	2.5	0.9544	107.929	0.781	1.3	0.275	78.9	NFC
		5	0.9137	145.618	0.765				
		7.5	0.8798	141.530	0.755				
		10	0.8541	120.104	0.753				
		12.5	0.8378	95.284	0.755				
17	313.15	2.5	0.9624	48.265	0.788	1.3	0.36	72.3	TI
		5	0.9296	69.164	0.773				
		7.5	0.9027	72.781	0.764				
		10	0.8827	67.575	0.760				
		12.5	0.8701	58.024	0.760				

[a] Refer to Table 4 for observing the data set number. Refer to the Supporting Information for observing all of the detailed consistency test results.

pseudoexperimental. But this is doubtful and seems to be incorrect for the data of the L_w-H region because there is possibility of structure change of the clathrate hydrate and these would result in inaccurate generated data. Apart from that, it is

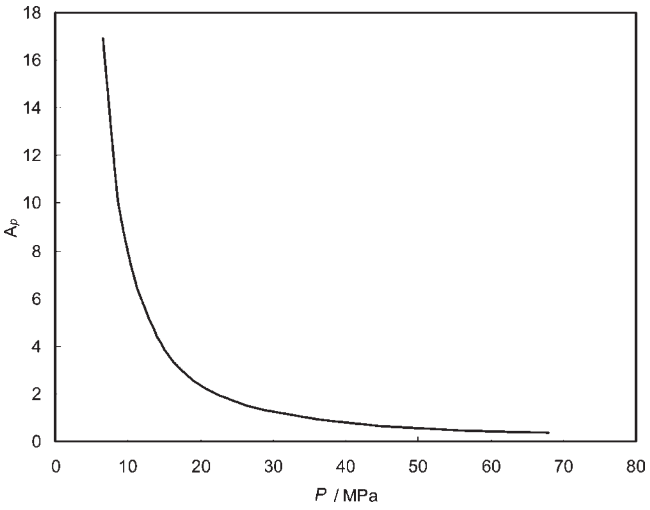

Figure 2. Typical evaluated integral in eq 5 for the data set 3 regarding the solubility of methane in water.

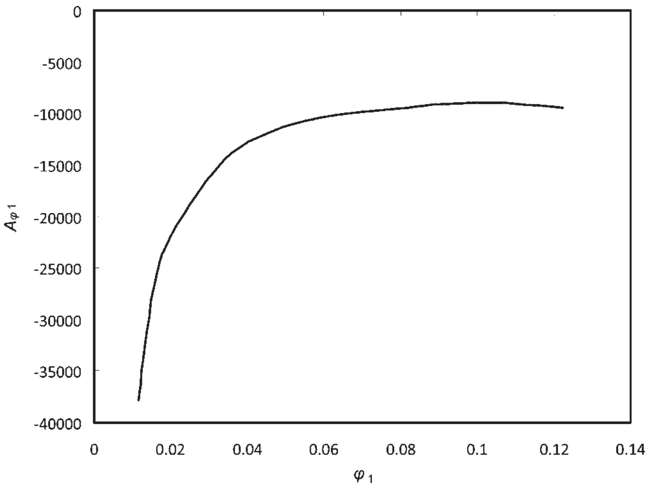

Figure 3. Typical evaluated integral in eq 7 for the data set 3 regarding the solubility of methane in water.

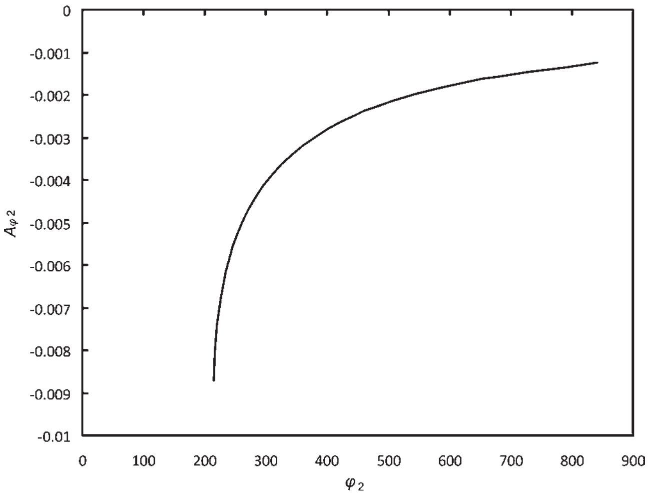

Figure 4. Typical evaluated integral in eq 8 for the data set 3 regarding the solubility of methane in water.

not recommended to generate data based on doubtful data, which are not yet thermodynamically tested. Therefore, one has to perform such a test with the existed experimental data, even if only two isothermal data points are available.

It should be noted that the investigated experimental data have been generated by different experimental techniques. In this work, we just focused on the extent that these data are thermodynamically consistent. More meticulous investigations should be made on the validity of the applied experimental techniques in future works.

■ CONCLUSIONS

The requirement of reliable experimental solubility data for the carbon dioxide/methane + water system is drastic especially in petroleum industry. In this work, a thermodynamic consistency test was applied on the related 49 isothermal experimental data sets inside and outside hydrate formation regions. The VPT EoS[38] with NDD mixing rules[39] was applied to predict the solubilities in the aforementioned systems for the L_w-G/V equilibrium region while another model based on van der Waals−Platteeuw[40] model and Henry's law was used for predictions of the solubilities in L_w-H equilibrium region. The consistency test was based on the area test approach derived from the original Gibbs−Duhem equation[21−25] at constant temperature.[26−32] For outside of hydrate formation region, the results show that around 47 % of the investigated experimental data of solubilities of carbon dioxide in water seem to be thermodynamically consistent; meanwhile, this percentage is about 53 % for inconsistent data and 0 % for not fully consistent data. These percentages are about 31 %, 46 %, and 23 % for the data of concentrations of carbon dioxide in the gas/vapor phase, respectively. Furthermore, around 16 % of the investigated experimental data of solubilities of methane in water seem to be thermodynamically consistent, while this percentage is about 78 % for inconsistent data and 6 % for not fully consistent data. These percentages are around 0 %, 50 %, and 50 % regarding the experimental data of concentrations of methane in gas phase, respectively. In addition, the results indicated that the measurements of such data must be done accurately and deliberately to be able to use in tuning of the future models for predictions/representation of such solubilities in different equilibrium conditions.

■ APPENDIX

In the thermodynamic model, the VPT EoS[38] is used for modeling fluid phases, as it is believed that this EoS is a strong tool for modeling systems containing water and polar compounds.[39] This EoS is written as follows:[38]

$$P = \frac{RT}{v-b} - \frac{a}{v(v+b)+c(v-b)} \tag{A.1}$$

with

$$a = \bar{a}\alpha(T_r) \tag{A.2}$$

$$\bar{a} = \frac{\Omega_a R^2 T_c^{\,2}}{P_c} \tag{A.3}$$

$$b = \frac{\Omega_b R T_c}{P_c} \tag{A.4}$$

$$c = \frac{\Omega_c R T_c}{P_c} \tag{A.5}$$

where the α function is given as:

$$\alpha(T_r) = [1 + F(1 - T_r^{\psi})]^2 \tag{A.6}$$

where $\psi = 0.5$ and the coefficient F is given by:

$$F = 0.43286 + 3.58230(\omega Z_c) + 8.1941(\omega Z_c)^2 \tag{A.7}$$

The subscripts c and r in the preceding equations denote critical and reduced properties, respectively, and ω is the acentric factor. Besides, the coefficients Ω_a, Ω_b, and Ω_c are calculated by:

$$\Omega_a = 0.66121 - 0.76105Z_c \tag{A.8}$$

$$\Omega_b = 0.02207 + 0.20868Z_c \tag{A.9}$$

$$\Omega_c = 0.57765 - 1.87080Z_c \tag{A.10}$$

where Z_c is the critical compressibility factor. Avlonitis et al.[37] relaxed the constraints on F and Ψ for water to improve the predicted vapor pressure and saturated volume for these compounds:

$$F = 0.72318 \qquad \Psi = 0.52084 \tag{A.11}$$

Later, Tohidi-Kalorazi[34] relaxed the alpha function for water, $\alpha_w(T_r)$, using experimental water vapor pressure data in the range of 258.15 to 374.15 K, in order to improve the predicted water fugacity:

$$\alpha_w(T_r) = 2.4968 - 3.0661T_r + 2.7048T_r^{\,2} - 1.2219T_r^{\,3} \tag{A.12}$$

Nonpolar−nonpolar binary interactions in fluid mixtures are described by applying classical mixing rules as follows:

$$a = \sum_i \sum_j z_i z_j a_{ij} \tag{A.13}$$

$$b = \sum_i z_i b_i \tag{A.14}$$

$$c = \sum_i z_i c_i \tag{A.15}$$

$$a_{ij} = (1 - k_{ij})\sqrt{a_i a_j} \tag{A.16}$$

where z denotes the mole fraction of mixture and k_{ij} is the standard binary interaction parameter.

For polar-nonpolar interaction, however, the classical mixing rules are not satisfactory, and therefore more complicated mixing rules are necessary. In this work, the NDD mixing rules developed by Avlonitis et al.[39] were applied to describe mixing in the a-parameter:

$$a = a^{\mathrm{C}} + a^{\mathrm{A}} \tag{A.17}$$

where a^{C} is given by the classical quadratic mixing rules (eqs A.13 and A.16). The term a^{A} corrects for asymmetric interaction which cannot be efficiently accounted for by classical mixing rules:[39]

$$a^{\mathrm{A}} = \sum_p z_p^{\,2} \sum_i z_i a_{pi} l_{pi} \tag{A.18}$$

$$a_{pi} = \sqrt{a_p a_i} \tag{A.19}$$

$$l_{pi} = l_{pi}^0 - l_{pi}^1(T - T_0) \tag{A.20}$$

where p is the index of polar components, and l represents the binary interaction parameter for the asymmetric term. The interaction parameters of the applied model have been reported by Tohidi-Kalorazi.[34]

Using the above EoS[38] and the associated mixing rules,[39] the fugacity of each component in fluid phases is calculated from:

$$f_i = z_i \varphi_i P \tag{A.21}$$

where φ_i is the fugacity coefficient of component i in the related phase. The fugacity coefficient of each component in fluid phase is derived straightforward from the following relation:[21−25,36]

$$\ln \varphi_i = \frac{1}{RT}\int_V^{\infty}\left[\left(\frac{\partial P}{\partial n_i}\right)_{T,V,n_{j\neq i}} - \frac{RT}{V}\right]\mathrm{d}V - \ln Z \tag{A.22}$$

■ ASSOCIATED CONTENT

Ⓢ Supporting Information. All of the results of the calculated/predicted solubilities and thermodynamic consistency tests of the investigated systems. This material is available free of charge via the Internet at http://pubs.acs.org.

■ AUTHOR INFORMATION

Corresponding Author

*E-mail: amir-hossein.mohammadi@mines-paristech.fr. Tel.: + (33) 1 64 69 49 70. Fax: + (33) 1 64 69 49 68.

Funding Sources

The financial support of the Agence Nationale de la Recherche (ANR) through the SECOHYA project and OSEM (Orientation Stratégique des Ecoles des Mines) is gratefully acknowledged. A.E. wishes to thank MINES ParisTech for providing a Ph.D. scholarship.

■ ACKNOWLEDGMENT

The authors are grateful to Prof. José O. Valderrama for the fruitful discussions done on the issue.

■ NOMENCLATURE

A= area (m^2) or parameter of Henry's constant correlation in eq 29
ARD= absolute relative deviation, %
a= attractive parameter of the equation of state ($\mathrm{MPa \cdot m^6 \cdot mol^{-2}}$) or parameter of Langmuir constant correlation in eq 26
$\bar{a}$= parameter of equation of state defined by eq A.3
B= parameter of Henry's constant correlation in eq 29
b= repulsive parameter of the equation of state ($\mathrm{m^3 \cdot mol^{-1}}$) or parameter of Langmuir constant correlation in eq 26
C= Langmuir constant (reciprocal MPa)
$\bar{C}$= parameter of Henry's constant correlation in eq 29
c= third parameter of the equation of state, ($\mathrm{m^3 \cdot mol^{-1}}$) or parameter of Langmuir constant correlation in eq 27
D= parameter of Henry's constant correlation in eq 29
d= parameter of Langmuir constant correlation in eq 27
d= derivative operator
E= error and equilibria
EOR= enhanced oil recovery
F= coefficient of the equation of state defined by eq A.7
f= fugacity (MPa)
G= gas
H= hydrate and Henry's constant defined by eq 29
k= binary interaction parameter
L= liquid
l= binary interaction parameter for the asymmetric term of VPT-EoS[38]
N= number of experimental data points
NDD= nondensity-dependent mixing rules[39]
NFC= not fully consistent data
P= pressure, (MPa)
R= universal gas constant, ($\mathrm{MPa.m^3/mol.K}$)
T= temperature, (K)
TC= thermodynamically consistent data
TI= thermodynamically inconsistent data
V= vapor or total volume
VPT-EoS= Valderrama modification of the Patel and Teja equation of state[38]
v= molar volume, ($\mathrm{m^3/mol}$)
v'= number of cavities per water molecule in a unit hydrate cell
x= mole fraction in liquid phase
y= mole fraction in gas/vapor phase
Z= compressibility factor
z= mole fraction of mixture (vapor/gas and liquid phases)

Greek Letters

α= alpha function of the equation of state
γ= activity coefficient
φ= fugacity coefficient
Δ= difference value
Ψ= coefficient used in eq A.6
ω= acentric factor
Ω= coefficients defined by eqs A.8 to A.10
μ= chemical potential
∂= partial derivative operator

Subscripts

A= area
a= attractive parameter of the EoS in eq A.8
b= repulsive parameter of the EoS in eq A.9
c= critical state c = or refers to the third parameter of the EoS in eq (A.10)
HC= hydrocarbon hydrate former
HF= hydrate former (carbon dioxide and methane)
i= ith component in a mixture or ith experimental data set
j= jth component in a mixture or jth individual calculated area
large= large type of cavities in water molecule
min= minimum
max= maximum
p= refers to experimental $P-T-z$ data and the index of polar components
r= reduced property
small= small type of cavities in water molecule
w= water
φ= refers to calculated parameters of the model for evaluations of the integrals in eqs 6-8
0= reference value
1= refers to water and the integral in eq 7
2= refers to methane/$\mathrm{CO_2}$

Superscripts

A= refers to asymmetric interaction

C= attractive term of the VPT-EoS[38] defined by classical quadratic mixing rules
calc= calculated value
E= excess property
exp= experimental value
H= hydrate
G= gas state
L= liquid state
MT= hypothetical empty hydrate lattice
pred= predicted value
sat= saturated state
V= vapor state
Ψ= parameter in eq A.6
0= first parameter of asymmetric binary interaction parameter
1= second parameter of asymmetric binary interaction parameter

REFERENCES

(1) Chapoy, A.; Mohammadi, A. H.; Chareton, A.; Tohidi, B.; Richon, D. Measurement and modeling of gas solubility and literature review of the properties for the carbon dioxide-water system. *Ind. Eng. Chem. Res.* **2004**, *43*, 1794–1802.

(2) Mohammadi, A. H.; Richon, D. Development of predictive techniques for estimating liquid water-hydrate equilibrium of water-hydrocarbon system. *J. Thermodyn.* **2009**, 1–12.

(3) Sloan, E. D. *Clathrate Hydrates of Natural Gases*, 2nd ed.; Marcel Dekker, Inc.: New York, 1998.

(4) Mohammadi, A. H.; Richon, D. Thermodynamic model for predicting liquid water-hydrate equilibrium of the water-hydrocarbon system. *Ind. Eng. Chem. Res.* **2008**, *47*, 1346–1350.

(5) Mohammadi, A. H.; Richon, D. Extension of a thermodynamic model to predict the liquid water - hydrate equilibrium of carbon dioxide - water system CO_2. *Personal Communication*, 2008.

(6) Mohammadi, A. H.; Richon, D. A mathematical model based on artificial neural network technique for estimating liquid water-hydrate equilibrium of water-hydrocarbon system. *Ind. Eng. Chem. Res.* **2008**, *47*, 4966–4970.

(7) Hashemi, Sh.; Macchi, A.; Bergeron, S.; Servio, Ph. Prediction of methane and carbon dioxide solubility in water in the presence of hydrate. *Fluid Phase Equilib.* **2006**, *246*, 131–136.

(8) Yang, S. O.; Yang, I. M.; Kim, Y. S.; Lee, C. S. Measurement and prediction of phase equilibria for water + CO_2 in hydrate forming conditions. *Fluid Phase Equilib.* **2000**, *175*, 75–89.

(9) Yang, S. O.; Cho, S. H.; Lee, H.; Lee, C. S. Measurement and prediction of phase equilibria for water + methane in hydrate forming conditions. *Fluid Phase Equilib.* **2001**, *185*, 53–63.

(10) Servio, P.; Englezos, P. Effect of temperature and pressure on the solubility of carbon dioxide in water in the presence of gas hydrate. *Fluid Phase Equilib.* **2001**, *190*, 127–134.

(11) Servio, Ph.; Englezos, P. Measurement of dissolved methane in water in equilibrium with its hydrate. *J. Chem. Eng. Data* **2002**, *47*, 87–90.

(12) Kim, Y. S.; Ryu, S. K.; Yang, S. O.; Lee, C. S. Liquid water-hydrate equilibrium measurements and unified predictions of hydrate-containing phase equilibria for methane, ethane, propane, and their mixtures. *Ind. Eng. Chem. Res.* **2003**, *42*, 2409–2414.

(13) Handa, Y. P. Effect of hydrostatic pressure and salinity on the stability of gas hydrated. *J. Phys. Chem.* **1990**, *94*, 2652–2657.

(14) Zatsepina, O. Ye.; Buffet, B. A. Phase equilibrium of gas hydrate: implications for the formation of hydrate in the deep sea floor. *Geophys. Res. Lett.* **1997**, *24/13*, 1567–1570.

(15) Ballard, A. L.; Sloan, E. D. The next generation of hydrate prediction: I. Hydrate standard states and incorporation of spectroscopy. *Fluid Phase Equilib.* **2002**, *194−197*, 371–383.

(16) Ballard, A. L. A non-ideal hydrate solid solution model for a multi-phase equilibria program. Ph.D. Thesis, Colorado School of Mines, Golden, CO, 2002.

(17) Yang, S. O. Measurements and predictions of phase equilibria for water + natural gas components in hydrate-forming conditions. Ph.D. Thesis, Korea University, December 2000.

(18) Seo, Y.; Lee, H.; Ryu, B. J. Hydration number and two-phase equilibria of CH_4 hydrate in the deep ocean sediments. *Geophys. Res. Lett.* **2002**, *29*, Article Number: 1244.

(19) Chou, I. M.; Burruss, R. C. *Personal Communication*, Dec 18, 2006 (quoted in ref 3).

(20) Gaudette, J.; Servio, P. Measurement of dissolved propane in water in the presence of gas hydrate. *J. Chem. Eng. Data* **2007**, *52*, 1449–1451.

(21) Prausnitz, J. M.; Lichtenthaler, R. N.; Gomez de Azevedo, E. *Molecular Thermodynamics of Fluid Phase Equilibria*; Prentice-Hall, Inc.: Upper Saddle River, NJ, 1999.

(22) Smith, J. M.; Van Ness, H. C.; Abbott, M. M. *Introduction to Chemical Engineering Thermodynamics*, 6th ed.; McGraw-Hill: New York, 2003.

(23) Van Ness, H. C.; Abbott, M. M. *Classical Thermodynamics of Non-electrolyte Solutions*; McGraw-Hill, New York, 1982.

(24) Raal, J. D. ; Mühlbauer, A. L.; *Phase Equilibria: Measurement and Computation*; Washington: Taylor & Francis, 1998.

(25) Poling, B. E.; Prausnitz, J. M.; O'Connell, J. P. *The Properties of Gases and Liquids*, 5th ed.; McGraw-Hill: New York, 2001.

(26) Valderrama, J. O.; Alvarez, V. H. A versatile thermodynamic consistency test for incomplete phase equilibrium data of high-pressure gas−liquid mixtures. *Fluid Phase Equilib.* **2004**, *226*, 149–159.

(27) Valderrama, J. O.; Robles, P. A. Thermodynamic consistency of high pressure ternary mixtures containing a compressed gas and solid solutes of different complexity. *Fluid Phase Equilib.* **2006**, *242*, 93–102.

(28) Valderrama, J. O.; Zavaleta, J. Thermodynamic consistency test for high pressure gas−solid solubility data of binary mixtures using genetic algorithms. *J. Supercrit. Fluids* **2006**, *39*, 20–29.

(29) Valderrama, J. O.; Reátegui, A.; Sanga, W. E. Thermodynamic consistency test of vapor-liquid equilibrium data for mixtures containing ionic liquids. *Ind. Eng. Chem. Res.* **2008**, *47*, 8416–8422.

(30) Valderrama, J. O.; Faúndez, C. A. Thermodynamic consistency test of high pressure gas−liquid equilibrium data including both phases. *Thermochim. Acta* **2010**, *499*, 85–90.

(31) Eslamimanesh, A.; Mohammadi, A. H.; Richon, D. Thermodynamic consistency test for experimental data of water content of methane. *AIChE J.* **2011**, in press.

(32) Eslamimanesh, A.; Mohammadi, A. H.; Richon, D. Thermodynamic consistency test for experimental data of sulfur content of hydrogen sulfide. *Ind. Eng. Chem. Res.* **2011**, *50*, 3555–3563.

(33) Bertucco, A.; Barolo, M.; Elvassore, N. Thermodynamic consistency of vapor-liquid equilibrium data at high pressure. *AIChE J.* **1997**, *43*, 547–554.

(34) Tohidi-Kalorazi, B. Gas hydrate equilibria in the presence of electrolyte solutions. Ph.D. Thesis, Department of Petroleum Engineering, Heriot-Watt University, Edinburgh, UK, 1995.

(35) Heriot−Watt University Hydrate model, version 1.1 (accessed June 2007) http://www.pet.hw.ac.uk/.

(36) Mohammadi, A. H.; Anderson, R.; Tohidi, B. Carbon monoxide clathrate hydrates: equilibrium data and thermodynamic modeling. *AIChE J.* **2005**, *51*, 2825–2833.

(37) Avlonitis D. Thermodynamics of gas hydrate equilibria. Ph.D. Thesis, Department of Petroleum Engineering, Heriot-Watt University, Edinburgh, UK, 1992.

(38) Valderrama, J. O. A generalized Patel-Teja equation of state for polar and non-polar fluids and their mixtures. *J. Chem. Eng. Jpn.* **1990**, *23*, 87–91.

(39) Avlonitis, D.; Danesh, A.; Todd, A. C. Prediction of VL and VLL equilibria of mixtures containing petroleum reservoir fluids and methanol with a cubic EoS. *Fluid Phase Equilib.* **1994**, *94*, 181–216.

(40) van der Waals, J. H.; Platteeuw, J. C. Clathrate solutions. *Adv. Chem. Phys.* **1959**, *2*, 1–57.

(41) von Stackelberg, M.; Muller, H. R. Feste Gashydrate. *Z. Elektrochem.* **1954**, *58*, 25.

(42) Parrish, W. R.; Prausnitz, J. M. Dissociation pressures of gas hydrate formed by gas mixture. *Ind. Eng. Chem. Process. Des. Dev.* **1972**, *11*, 26–34.

(43) Kihara, T. Virial coefficient and models of molecules in gases. *Rev. Mod. Phys.* **1953**, *25*, 831–843.

(44) McKoy, V.; Sinanoĝlu, O. Theory of dissociation pressures of some gas hydrates. *J. Chem. Phys.* **1963**, *38*, 2946–2956.

(45) Dharmawardhana, P. B.; Parrish, W. R.; Sloan, E. D. Experimental thermodynamic parameters for the prediction of natural gas hydrate dissociation conditions. *Ind. Eng. Chem. Fundam.* **1980**, *19*, 410–414.

(46) Chapoy, A.; Mohammadi, A. H.; Valtz, A.; Coquelet, C.; Richon, D. Water and Inhibitor Distribution in Gas Production Systems. GPA Research Project 987, RR-198; Tulsa, OK, 2008.

(47) Daubert, T. E.; Danner, R. P. *DIPPR Data Compilation Tables of Properties of Pure Compounds*; AIChE: New York, 1985.

(48) Constantinides, A.; Moustofi, N. *Numerical Methods for Chemical Engineers with MATLAB Applications*; Prentice Hall PTR: Upper Saddle River, NJ, 1999.

(49) Mickley, H. S.; Sherwood, T. K.; Reed, C. E. *Applied Mathematics in Chemical Engineering*; McGraw Hill: New York, 1957.

(50) Rao, S. S. *Applied Numerical Methods for Engineers and Scientists*; Prentice Hall: Upper Saddle River, NJ, 2002.

(51) Briones, J. A.; Mullins, J. C.; Thies, M. C.; Kim, B. U. Ternary phase equilibria for acetic acid-water mixtures with supercritical carbon dioxide. *Fluid Phase Equilib.* **1987**, *36*, 235–246.

(52) Nakayama, T.; Sagara, H.; Arai, K.; Saito, S. High pressure liquid-liquid equilibria for the system of water, ethanol and 1,1-difluoroethane at 323.2 K. *Fluid Phase Equilib.* **1987**, *38*, 109–127.

(53) Bamberger, A.; Sieder, G.; Maurer, G. High-pressure (vapor + liquid) equilibrium in binary mixtures of (carbon dioxide + water or acetic acid) at temperatures from 313 to 353 K. *J. Supercrit. Fluids* **2000**, *17*, 97–110.

(54) Malinin, S. D. The system water-carbon dioxide at high temperatures and pressures (in Russian). *Geokhimiya* **1959**, *3*, 292–306.

(55) Muller, G. Ph.D. Dissertation, University of Kaiserslautern, Kaiserslautern, Germany, 1983.

(56) Briones, J. A.; Mullins, J. C.; Thies, M. C.; Kim, B. U. Ternary phase equilibria for acetic acid-water mixtures with supercritical carbon dioxide. *Fluid Phase Equilib.* **1987**, *36*, 235–246.

(57) Takenouchi, S.; Kennedy, G. C. The binary system H_2O-CO_2 at high temperatures and pressures. *Am. J. Sci.* **1964**, *262*, 1055–1074.

(58) Servio, P.; Englezos, P. Effect of temperature and pressure on the solubility of carbon dioxide in water in the presence of gas hydrate. *Fluid Phase Equilib.* **2001**, *190*, 127–134.

(59) Yang, S. O.; Yang, I. M.; Kim, Y. S.; Lee, C. S. Measurement and prediction of phase equilibria for water+CO_2 in hydrate forming conditions. *Fluid Phase Equilib.* **2000**, *175*, 75–89.

(60) Culberson, O. L.; McKetta, J. J. The solubility of methane in water at pressures to 10000 psia. *AIME Pet. Trans.* **1951**, *192*, 223–226.

(61) Davis, J. E.; McKetta, J. J. Solubility of methane in water. *Petrol. Ref.* **1960**, *39*, 205–206.

(62) Lekvam, K.; Bishnoi, P. R. Dissolution of methane in water at low temperatures and intermediate pressures. *Fluid Phase Equilib.* **1997**, *131*, 297–309.

(63) Chapoy, A.; Mohammadi, A. H.; Richon, D.; Tohidi, B. Gas solubility measurement and modeling for methane—water and methane—ethane—n-butane—water systems at low temperature conditions. *Fluid Phase Equilib.* **2004**, *220*, 113–121.

(64) Yarym-Agaev, N. L.; Sinyavskaya, R. P.; Koliushko, I. I. Phase equilibrium in the binary systems water-methane and methanol-methane under high pressure (in Russian). *Zh. Prikl. Khim.* **1985**, *58*, 165–168.

(65) Sanchez, M.; De Meer, F. Equilibrio liquido-vapor del sistema metano-agua para altas presiones y temperaturas comprendidas entre 150 Y 300 °C. *Ann. Quim.* **1978**, *74*, 1325–1328.

(66) Sultanov, R. G.; Skripka, V. G.; Namiot, A. Y. Phase equilibria in the systems methane—n-hexadecane and nitrogen—n-hexadecane at high temperatures and pressures. *Viniti* **1971**, 2888–71.

(67) Yang, S. O.; Choa, S. H.; Leeb, H.; Lee, C. S. Measurement and prediction of phase equilibria for water + methane in hydrate forming conditions. *Fluid Phase Equilib.* **2001**, *185*, 53–63.

(68) Seo, Y.; Lee, H.; Uchida, T. Methane and carbon dioxide hydrate phase behavior in small porous silica gels: three-phase equilibrium determination and thermodynamic modeling. *Langmuir* **2002**, *18*, 9164–9170.

(69) Lu, W. J.; Chou, I. M.; Burruss, R. C.; Yang, M. Z. In situ study of mass transfer in aqueous solutions under high pressures via Raman Spectroscopy: A new method for the determination of diffusion coefficients of methane in water near hydrate formation conditions. *Appl. Spectrosc.* **2006**, *60*, 122–129.